Supplementary Text

Complete Hamiltonian

To derive the system Hamiltonian $\hat{H}$, we need the equations of motion for the atomic ensemble and the digital resonator separately. Assuming the Xe atoms are in a static magnetic field B_z, their motion can be described by the Bloch equation[1,2]:

$$\dot{\vec{\boldsymbol{M}}} = \vec{\omega} \times \vec{\boldsymbol{M}} - \frac{M_x}{T_2}\vec{x} - \frac{M_y}{T_2}\vec{y} + \frac{M_0 - M_z}{T_1}\vec{z}, \tag{1}$$

here, $\vec{\boldsymbol{M}}$ is the atomic polarization vector, and $\vec{\omega}$ is the Larmor precession angular velocity. In a magnetic field, $\vec{\omega} = \Gamma\vec{B}$, where Γ is the gyromagnetic ratio. $M_{x(y,z)}$ denotes the component of $\vec{\boldsymbol{M}}$ along the $x(y,z)$ axis, and M_0 is the magnitude of M_z at steady state. T_2 and T_1 are the transverse and longitudinal relaxation times, respectively. In this experiment, the probe light propagates along the y-axis. It interacts with Rb atoms to get their precession signal, and then extracts the signal of Xe atoms ($M_{x(y)}$) through signal demodulation. Since we measure $M_{x(y)}$, we only need to consider the effect of T_2.

Expanding $\vec{\boldsymbol{M}}$ in the Bloch equation (1) along the x, y, and z axes respectively, we obtain the following equations:

$$\dot{M}_x = \omega_y M_z - \omega_z M_y - \frac{M_x}{T_2}, \tag{2}$$

$$\dot{M}_y = \omega_z M_x - \omega_x M_z - \frac{M_y}{T_2}, \tag{3}$$

$$\dot{M}_z = \omega_x M_y - \omega_y M_x - \frac{M_0 - M_z}{T_1}. \tag{4}$$

By introducing $\boldsymbol{M}_+ = M_x - iM_y = M_\perp \cdot e^{i\varphi}$ in equations (2)-(4) and separating the imaginary and real parts, we can derive the following:

$$\dot{\boldsymbol{M}}_+ = \left(\omega_y + i\omega_x\right)M_z - \left(i\omega_z + \frac{1}{T_2}\right)\boldsymbol{M}_+. \tag{5}$$

In the experiment, M_y lies in the xy-plane and is 90° out of phase with M_x. Thus, we can denote $y_1 = \boldsymbol{M}_+$, and $x_1 = M_z\omega_x = M_z\Gamma B_x$ as the signal input caused by the magnetic field B_x from the x-axis coil. Here, $\omega_z = \omega_1$ represents the eigenfrequency of atomic precession, $\frac{1}{T_2} = \gamma_1$ indicates the atomic resonance loss, and $\omega_y = 0$ signifies no input along the y-axis. Assuming M_z remains constant during the experiment, equation (5) can be rewritten as follows.

$$\dot{y_1} = -(i\omega_1 + \gamma_1)y_1 + ix_1. \tag{6}$$

Equation (6) indicates that y_1 represents the polarization of Xe atoms within the xy-plane, which is the measured quantity. The signal, derived from equation (6), is an oscillating signal of the form $M_\perp cos(\omega_1 +$

$\phi_0)^2$, where ϕ_0 is the initial phase, ω_1 is the oscillation frequency, and $M_\perp$ is the signal amplitude. The loss γ_1 and input x_1 in equation (6) determine the variation of $M_\perp$. For subsequent discussion and calculation, y_1 continues to represent the output of the magnetometer.

Similarly, for the digital resonator, we can derive an analogous equation of motion, which is also governed by a second-order differential equation[3]:

$$\ddot{y_2} + 2\gamma_2\dot{y_2} + \omega_2^2 y_2 = 2\gamma_2\omega_2 x_2, \tag{7}$$

here, $x_2$and y_2 represent the input and output, ω_2 is the eigenfrequency, and γ_2 is the loss. Assuming the output signal is oscillatory, expressed as $y_2 = Ae^{-i\omega_2 t}$ (where *A* is the signal amplitude), substituting this into equation (7) and neglecting the slow-varying term $\ddot{A}e^{-i\omega_2 t}$, we obtain:

$$-2i\omega_2\dot{A}e^{-i\omega_2 t} - \omega_2^2 Ae^{-i\omega_2 t} + 2\gamma\dot{A}e^{-i\omega_2 t} - 2i\omega_2\gamma_2 Ae^{-i\omega_2 t} + \omega_2^2 Ae^{-i\omega_2 t} = 2\gamma_2\omega_2 x_2. \tag{8}$$

After simplification, the equation (8) becomes:

$$\dot{y_2} = -(i\omega_2 + \gamma_2)y_2 + \frac{\gamma_2^2}{\omega_2}x_2 + i\gamma_2 x_2. \tag{9}$$

Given that $\omega_2 \gg \gamma_2$, the term $\frac{\gamma_2^2}{\omega_2}x_2$ can be neglected. After normalizing the input term with respect to γ_2 , equation (9) simplifies to:

$$\dot{y_2} = -(i\omega_2 + \gamma_2)y_2 + ix_2, \tag{10}$$

whose form is identical to equation (6). Finally, they can be transformed into a Schrödinger-like form:

$$i\dot{y_{1,2}} = (\omega_{1,2} - i\gamma_{1,2})y_{1,2} - x_{1,2}. \tag{11}$$

Finally, by setting the inputs as a linear combination of the output signals, specifically $x_n = g_n(\kappa_1 e^{-i\theta}y_1 + \kappa_2 e^{-i\varphi}y_2)$, we can derive the Hamiltonian matrix:

$$\hat{H} = \begin{bmatrix} \omega_1 - i\gamma_1 - g_1\kappa_1 e^{-i\theta} & -g_1\kappa_2 e^{-i\varphi} \\ -g_2\kappa_1 e^{-i\theta} & \omega_2 - i\gamma_2 - g_2\kappa_2 e^{-i\varphi} \end{bmatrix}. \tag{12}$$

After shifting the matrix by $\frac{\omega_1+\omega_2}{2}$, we obtain:

$$\hat{H} = \begin{bmatrix} \nu - i\gamma_1 - g_1\kappa_1 e^{-i\theta} & -g_1\kappa_2 e^{-i\varphi} \\ -g_2\kappa_1 e^{-i\theta} & -\nu - i\gamma_2 - g_2\kappa_2 e^{-i\varphi} \end{bmatrix}, \tag{13}$$

where $\nu = \frac{\omega_1-\omega_2}{2}$. Finally, the full expression for the eigenvalues can be calculated from the matrix:

$$\lambda = \frac{1}{2}(-i\gamma_1 - g_1\kappa_1 e^{-i\theta} - i\gamma_2 - g_2\kappa_2 e^{-i\varphi} \pm \sqrt{(2\nu - i\gamma_1 - g_1\kappa_1 e^{-i\theta} + i\gamma_2 + g_2\kappa_2 e^{-i\varphi})^2 + 4g_1 g_2\kappa_1\kappa_2 e^{-i(\theta+\varphi)}}). \tag{14}$$

Signal processing

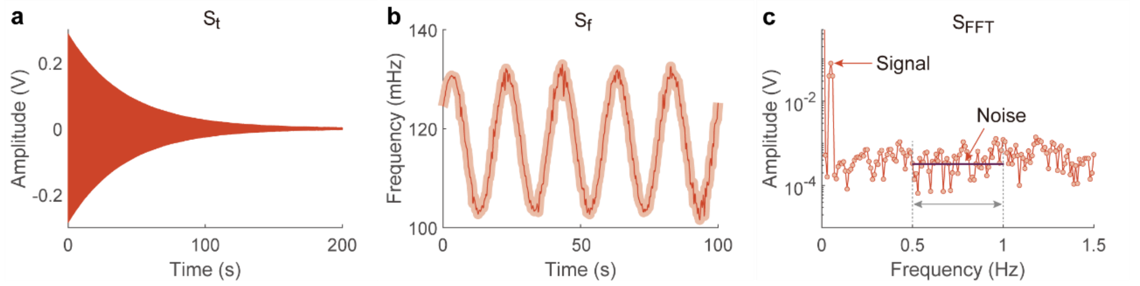

Fig. s1 | The signal processing

As shown in Figure s1a, the system's original output signal S_t is a damped oscillation signal:

$$S_t = A_0(t) \cdot e^{-\gamma t} \cos(\omega t), \tag{15}$$

where γ is the decay rate, ω is the frequency. When we modulate the magnetic field sinusoidally, the signal's frequency ω also oscillates accordingly. The first step in processing the signal is to use a lock-in amplifier to obtain the time-varying frequency ω, resulting in a frequency signal S_f. During the experiment, we applied periodic modulation to the magnetic field B_z, expressed as $B_z = B_0 \pm \delta B \cos(\Omega t)$, where δB is the modulation amplitude and $\Omega = 2\pi \cdot 0.05\text{Hz}$ is the modulation frequency. As depicted in Figure s1b, the frequency signal S_f obtained using a lock-in amplifier is a sine signal with the same period as the modulation signal. To ensure the original signal S_t has sufficient intensity, each data set was processed using only the first 100 seconds of the raw signal. Finally, as shown in Figure s1c, the time-domain frequency signal S_f is transformed into the frequency domain via FFT to obtain the spectrum S_{FFT}:

$$\mathcal{F}(S_f) = S_{FFT} \tag{16}$$

In the spectrum signal S_{FFT}, there's a clear peak at 0.05 Hz, matching the modulation frequency Ω of the magnetic field. The peak height represents the signal strength.

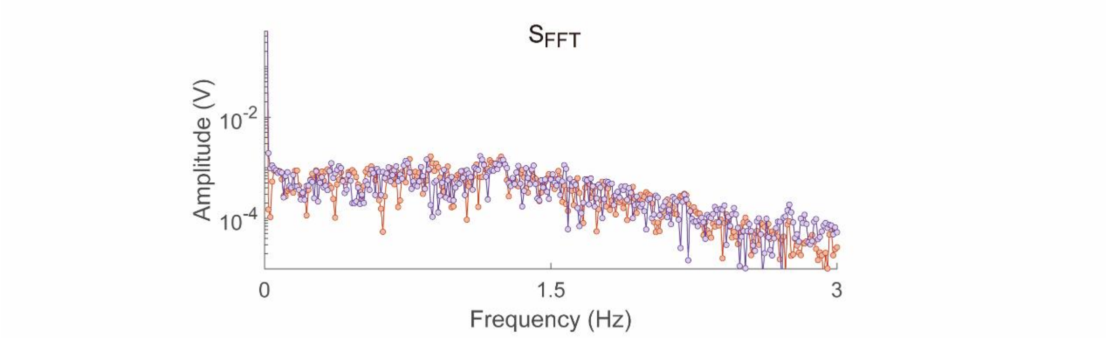

Fig. s2 | The background noise

The average spectrum between 0.5 Hz and 1 Hz indicates the noise level, which aligns well with the experimental conditions. As shown in Figure s2, to observe the system's noise enhancement effect, we measured the background noise of conventional atomic magnetometer (purple) and EP-enhanced magnetometer (orange). In the 0.05-1.2Hz band, the noise tends to flatten overall and shows no obvious frequency selectivity when amplified.

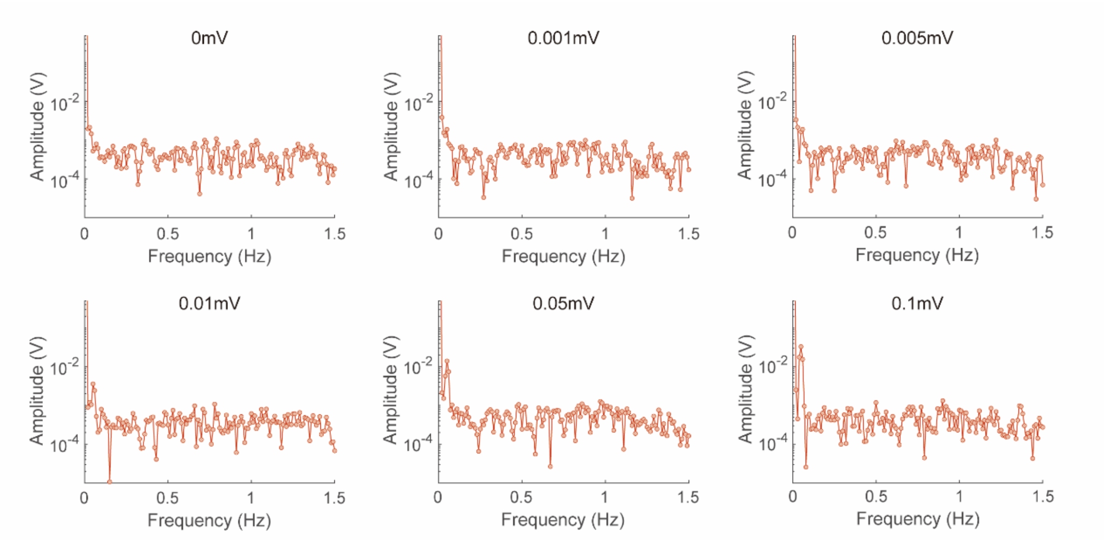

Fig. s3 | Noise of the EP-enhanced magnetometer with low input signal amplitudes

In Figure s3, as the input signal amplitude gradually increases from 0 mV to 0.1 mV, the noise of the EP-enhanced magnetometer in the 0.08–1.2 Hz band remains flat, consistent with the background noise characteristics. A signal peak begins to emerge at 0.05 Hz. To further validate the noise characteristics in the 0.08–1.2 Hz band, we calculated the noise enhancement of the EP-enhanced magnetometer relative to the conventional atomic magnetometer using two frequency bands (0.08–1 Hz and 0.5–1 Hz) at a signal amplitude of 0.1 mV. Results from five repeated experiments showed a noise enhancement of 1.33× and 1.36×, respectively, which indicate stable noise levels in these bands.

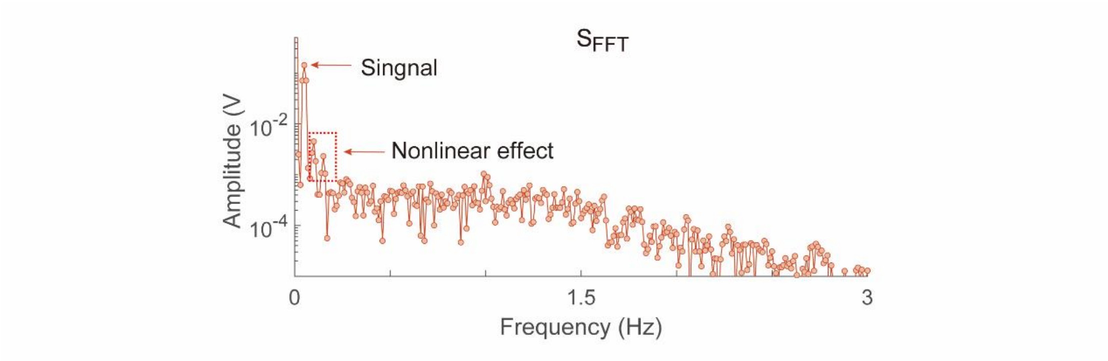

Fig. s4 | Noise of the EP-enhanced magnetometer with high input signal amplitudes (0.5mV)

As the modulation amplitude increases, the noise characteristics in the low-frequency region begin to change. In Figure s4, high modulation amplitudes (0.5mV) caused multiple harmonic peaks near the signal due to the nonlinear response near the EP. To avoid such interference, we chose the 0.5-1Hz band for noise evaluation.

References

1 Budker, D. & Jackson Kimball, D. F. *Optical Magnetometry*. (Cambridge University Press, 2013).

2 Walker, T. G. & Larsen, M. S. in *Advances In Atomic, Molecular, and Optical Physics* Vol. 65 (eds Ennio Arimondo, Chun C. Lin, & Susanne F. Yelin) 373-401 (Academic Press, 2016).

3 Oppenheim, A. V. & Willsky, A. S. *Signals and systems*. (Prentice-Hall, 1983).